

Catalytic co-pyrolysis of torrefied poplar wood and high-density polyethylene over hierarchical HZSM-5 for mono-aromatics production

Xiaona Lin ^a, Lingshuai Kong ^a, Xiajin Ren ^a, Donghong Zhang ^a, Hongzhen Cai ^{a,*}, Hanwu Lei ^{b,**}

^a School of Agricultural Engineering and Food Science, Shandong University of Technology, Zibo, 255000, China

^b Department of Biological Systems Engineering, Washington State University, Richland, WA, 99352, USA



ARTICLE INFO

Article history:

Received 29 April 2020

Received in revised form

24 August 2020

Accepted 14 September 2020

Available online 18 September 2020

Keywords:

Torrefaction

Co-pyrolysis

Hierarchical HZSM-5

Biomass

Mono-aromatics

ABSTRACT

The catalytic co-pyrolysis of torrefied poplar wood sawdust (TPW) and high-density polyethylene (HDPE) was investigated over hierarchical HZSM-5. Compared with raw PW/HDPE, the bio-oil yield from co-pyrolysis of TPW/HDPE decreased gradually while the quality of bio-oil was upgraded. With increasing torrefaction temperature from 220 to 280 °C, the amounts of acids, furans, and anhydrosugars in bio-oil were significantly reduced due to the removal of hemicellulose, whereas the production of phenols and alkenes were improved due to the enhanced hydrogen transfer reaction. In the catalytic co-pyrolysis, increasing torrefaction temperature caused an enhanced production of mono-aromatics as well as the selectivity of BTX (benzene, toluene, and xylene). Nevertheless, severe torrefaction (280 °C) lead to a rapid reduction of aromatic yield and selectivity due to the loss of cellulose. Compared to parent HZSM-5, hierarchical HZSM-5 treated with alkaline concentration (0.2–0.3 mol/L) favored the formation of mono-aromatics at the expense of polyaromatics. The maximum mono-aromatics yield of 71.75% was obtained during catalytic co-pyrolysis of 260-TPW/HDPE over 0.3-HZSM-5. The present work suggests that torrefaction pretreatment followed by the catalysis of hierarchical HZSM-5 is an efficient way to promote the production of valuable mono-aromatic hydrocarbons from biomass and plastic wastes.

© 2020 Elsevier Ltd. All rights reserved.

1. Introduction

Renewable resources have gained increasing attention worldwide due to the shortage of fossil fuels and environment pollution. Biomass is an abundant, low-cost, and eco-friendly energy source and can be directly converted into liquid fuels through fast pyrolysis, which is considered as a promising alternative to fossil fuels [1,2]. However, the pyrolysis oil obtained from biomass, known as bio-oil, has some undesirable properties such as corrosive, unstable, low heating value, and incompatible with fossil fuel, limiting its use in conventional engines and boilers [3]. Incorporation of hydrogen-rich materials such as thermoplastics into biomass pyrolysis process can enhance the quality of the end-product bio-oil [4,5]. It is reported that more than 300 million tons of plastics are

produced annually worldwide [6]. The continuous increase of waste plastics needs to be disposed harmlessly. Thereby, co-pyrolysis of plastic waste with biomass is an efficient method to mitigate plastic pollution and simultaneously obtain value-added liquid fuels [7].

Torrefaction, as one of the main pretreatment ways of biomass, is an effective technique to gain an improved quality of bio-oil by reducing oxygen content. Torrefaction is a thermal pretreatment to increase biomass energy density and remove water from biomass at the temperature ranging from 200 to 300 °C [8,9]. During the torrefaction of biomass, part of the hemicellulose and the branches of cellulose and lignin are eliminated from biomass as volatile vapors, enhancing the pyrolysis characteristics of biomass [10]. Torrefaction pretreatment has been demonstrated to cause the deoxygenation of biomass feedstock and facilitate aromatic production [11–14]. Aromatics, especially mono-aromatics such as benzene, toluene, and xylenes (BTXs), are important chemical materials [15,16]. Thus, it is crucial to increase the content of aromatic

* Corresponding author.

** Corresponding author.

E-mail addresses: chzh66666@126.com (H. Cai), hlei@wsu.edu (H. Lei).

compounds in bio-oil for its use as fuel additives or value-added chemical production. Several researchers have reported that torrefaction pretreatment can increase the yields of aromatics in the bio-oil from the co-pyrolysis of biomass and plastics [17,18], which confirmed that the combination of torrefaction and co-pyrolysis is a promising strategy. Recently, the effects of factors such as co-pyrolysis temperature and catalyst type/amount on the production of aromatic hydrocarbons through catalytic fast pyrolysis of torrefied biomass and plastics have been studied [6,19]. For example, Park et al. [19] investigated the effect of catalyst properties on the aromatic production during catalytic co-pyrolysis of torrefied yellow poplar and high-density polyethylene (HDPE). They summarized that both the large pore size and strong acidity of the catalyst were important for aromatics production. However, little attention has been focused on the effect of torrefaction pretreatment conditions (e.g. torrefaction temperature and time) on the aromatic production during catalytic co-pyrolysis of biomass and plastics.

Over the past decades, a lot of catalysts have been tested in the catalytic co-pyrolysis process ranging from zeolites [20,21], metal oxides [22], acidic mesoporous materials [23], carbon-based materials [24], etc. Among these, HZSM-5 zeolite is found to be the most frequently used and the most effective catalyst in aromatic production due to its unique pore structure and relatively strong acidity. However, the micropores of HZSM-5 zeolite severely hindered the diffusion of bulky compounds causing coke deposition on the surface and reducing catalyst efficiency, which is a well-known issue in the HZSM-5 upgrading process. Moreover, the undesirable polymerization of aromatic hydrocarbon precursors at the acid sites of HZSM-5 zeolite resulted in the high polyaromatic hydrocarbons (PAHs) yield [25,26]. Fortunately, this hindering diffusion effect could be reduced by introducing mesopores connected to micropores in the HZSM-5 zeolite. Hierarchical HZSM-5 zeolite containing both micropores and mesopores can be prepared by alkaline treatment that involves partial desilication of the HZSM-5 framework to generate larger pore openings and higher external surface area. The incorporation of mesopores in the HZSM-5 zeolite was found to improve the catalytic activity by decreasing the diffusion and accessibility limitation of bulky molecules in petrochemical and biomass upgrading process [27]. For example, Li et al. [28] prepared a series of mesoporous HZSM-5 zeolites with varying alkaline concentrations, finding that hierarchical HZSM-5 improved the diffusion of bulky oxygenates and produced more aromatic hydrocarbons and less coke compared to the parent HZSM-5 in catalytic pyrolysis of beech wood. Chen et al. [29] also reported that suitable mesopores of HZSM-5 zeolite created by alkaline treatment enhanced mass transfer efficiency, increasing the yield of aromatics in catalytic pyrolysis of rice straw. Thus, the hierarchical HZSM-5 zeolite is hypothesized to improve the aromatic production during co-pyrolysis of torrefied biomass and plastics.

Poplar wood (PW) is one of the widespread and abundant species in China, which can be used for timbers and furniture. Consequently, large amounts of PW sawdust and residues are generated every year. In this study, to obtain a high content of valuable mono-aromatics in the bio-oil, PW was first pretreated by torrefaction and then was catalytically co-pyrolyzed with HDPE in the presence of hierarchical HZSM-5 zeolite by using a fixed bed reactor. The torrefaction temperatures of PW (220, 240, 260, and 280 °C) and concentrations of alkaline treated HZSM-5 zeolite (0.2, 0.3, and 0.4 mol/L) were studied to obtain their effects on mono-aromatic hydrocarbons production. The influence of combining the torrefaction pretreatment with hierarchical HZSM-5 catalysis on the mono-aromatic formation mechanism was proposed.

2. Materials and methods

2.1. Materials

PW, obtained from Heilongjiang, China, was smashed in a high-speed rotary cutting mill and screened to the particle size of 200–400 μm , then dried at 105 °C for 48 h. HDPE (particle size 250–500 μm) was purchased from Tianjin Petrochemical Company, China. HZSM-5 zeolite (powder, Si/Al = 35) was purchased from Nankai University Catalyst Co., Ltd., China. The zeolite was calcined at 550 °C for 5 h before use. NaOH and NH_4NO_3 were purchased from Tianjin Hengxing Chemical Co., Ltd., China.

2.2. Torrefaction of PW

The torrefaction of PW was conducted in a tube furnace. PW (5 g) was placed into the furnace at room temperature, and then a nitrogen flow of 40 mL/min was used to remove oxygen. After that, the PW was heated from room temperature to the desired temperatures (220, 240, 260 and 280 °C) with the heating rate of 5 °C/min, and hold on for 20 min. After the treatment, samples were cooled to room temperature and then were stored in a desiccator for use. The torrefied sample was labeled as χ -TPW, where χ is the torrefaction temperature. The ultimate analysis of TPW was determined using an elemental analyzer (Euro EA3000, Italy). The chemical components of raw and TPW were conducted in a semi-automatic fiber analyzer (ANKOM A200i, USA).

2.3. Hierarchical HZSM-5 preparation and characterization

The hierarchical HZSM-5 zeolites were prepared using the following method: 5 g HZSM-5 zeolite was added into 100 mL NaOH solution (0.2, 0.3, and 0.4 mol/L), and was heated at 80 °C for 1 h. After treatment, the samples were filtrated and washed by deionized water three times, and then dried at 105 °C for 6 h. The treated zeolites were ion-exchanged in 100 mL NH_4NO_3 solution (0.1 mol/L) at 80 °C for 1 h three times and were finally calcinated at 550 °C for 5 h. The prepared hierarchical HZSM-5 zeolite was denoted as χ -HZSM-5, where χ was the concentration of NaOH solution.

XRD analysis of the catalysts was conducted using a Bruker AXS D8 Advance X-ray diffractometer (Germany). The diffracted intensity of Cu-K α radiation was 40 kV and 40 mA, and the diffraction angle was in the range of 3–60° with the scanning rate of 2°/min. BET was determined using a Micromeritics ASAP 2020 instrument at an operating temperature of –196 °C. The sample was degassed at 300 °C for 3 h prior to analysis. The multipoint Brunauer-Emmett-Teller (BET) method was used to determine the specific surface area, and the pore volume and diameter were determined by the Barrett-Joyner-Halenda (BJH) method. NH_3 -TPD was carried out on an AutoChem II 2920 apparatus (Micromeritics, USA) to measure the acidity of the catalyst. Typically, about 50 mg catalyst was heated at 550 °C in a He flow (30 mL/min) for 1 h and then cooled to 100 °C, followed by NH_3 adsorption under 15 vol% NH_3/He flow (30 mL/min) for 0.5 h. The NH_3 -TPD was performed in the temperature range from 100 to 700 °C.

2.4. Thermogravimetric analysis

The co-pyrolysis behaviors of TPW and HDPE mixture with or without catalyst were performed using a Netzsch STA449F5 thermogravimetric analysis (TGA). The sample (5 mg) was decomposed under 20 mL/min N_2 flow from room temperature to 800 °C with a heating rate of 10 °C/min. The kinetic results are shown in Supplementary material.

2.5. Co-pyrolysis experiment

The catalytic co-pyrolysis experiments were performed on a drop tube reactor (Fig. 1) with an internal diameter and height of 22 and 400 mm, respectively. Once the pyrolysis tube was heated to 550 °C with 100 mL/min nitrogen as the carrier gas, 3 g TPW and HDPE mixture with the ratio of 1 was dropped into the reactor and hold for 20 min to ensure complete pyrolysis. Approximately 3 g catalyst was placed in the catalyst bed. The carrier gas carried the pyrolysis vapors through the catalyst bed and then entered a cooling condenser, containing two quartz glass tubes with ethylene glycol submerged in a liquid bath (−10 °C). After the reactor cooled to the room temperature, the solid residue in the pyrolysis tube was collected and weighed. The yield of bio-oil was calculated by weighing the difference between the condenser before and after pyrolysis. The coke on the catalyst was obtained by weighing the mass difference of catalyst before and after pyrolysis. The gas yield was calculated by difference.

The collected liquids were semi-quantitatively analyzed by an Agilent 6890N gas chromatograph (GC) connecting with an Agilent 5973 mass spectrometry (GC-MS). About 1 μL liquid was injected into GC-MS using 7683 series auto-injector. The injection temperature was set to 280 °C and the pyrolysis products were separated on an Agilent DB-1701 capillary column (60 m × 0.25 mm × 0.25 μm). The split ratio was 60:1 with a constant helium carrier gas flow of 1 mL/min. The oven was held at an initial temperature of 40 °C for 2 min, then programmed to 240 °C at a heating rate of 5 °C/min and hold for 5 min. All the compounds were identified by comparing their spectrograms with those from the National Institute of Standards and Technology mass spectral data library.

3. Results and discussion

3.1. Properties of TPW

The ultimate and proximate analyses of raw and torrefied PW are shown in Table 1. When the torrefaction temperature increased, the carbon content of TPW was increased at the expense of oxygen, resulting in lower O/C ratios. It is evident that torrefaction pre-treatment caused deoxygenation of PW as the main reactions. Oxygen was released in the form of H₂O, CO₂, CO, and some organic volatiles via dehydration, decarboxylation, and decarbonylation reactions [30]. The volatile content of PW was not significantly different from TPW at the torrefaction temperature of 220 °C, whereas a remarkable reduction was observed with further increasing torrefaction temperatures. The volatile content of TPW eventually decreased by 11% at the torrefaction temperature of

Table 1
Properties of raw PW, TPW, and HDPE.

Sample	PW	220-PW	240-PW	260-PW	280-PW	HDPE
Ultimate analysis (% dry and ash free)						
C	48.63	48.63	50.51	51.71	53.68	85.34
H	6.08	6.02	6.47	5.95	5.75	12.22
O (by difference)	44.4	44.52	42.15	41.36	39.5	2.44
N	0.24	0.18	0.19	0.2	0.22	0
Proximate analysis (% dry base)						
Volatiles	85.73	85.11	82.67	79.71	75.99	100
Ash	0.65	0.65	0.68	0.78	0.85	0
Fixed carbon	13.62	14.24	16.65	19.51	23.16	0
Component analysis (%)						
Cellulose	52.06	48.36	52.66	49.49	51.28	
Hemicellulose	17.24	16.96	9.38	0.18	0.13	
Lignin	16.78	17.33	23.57	39.51	40.83	

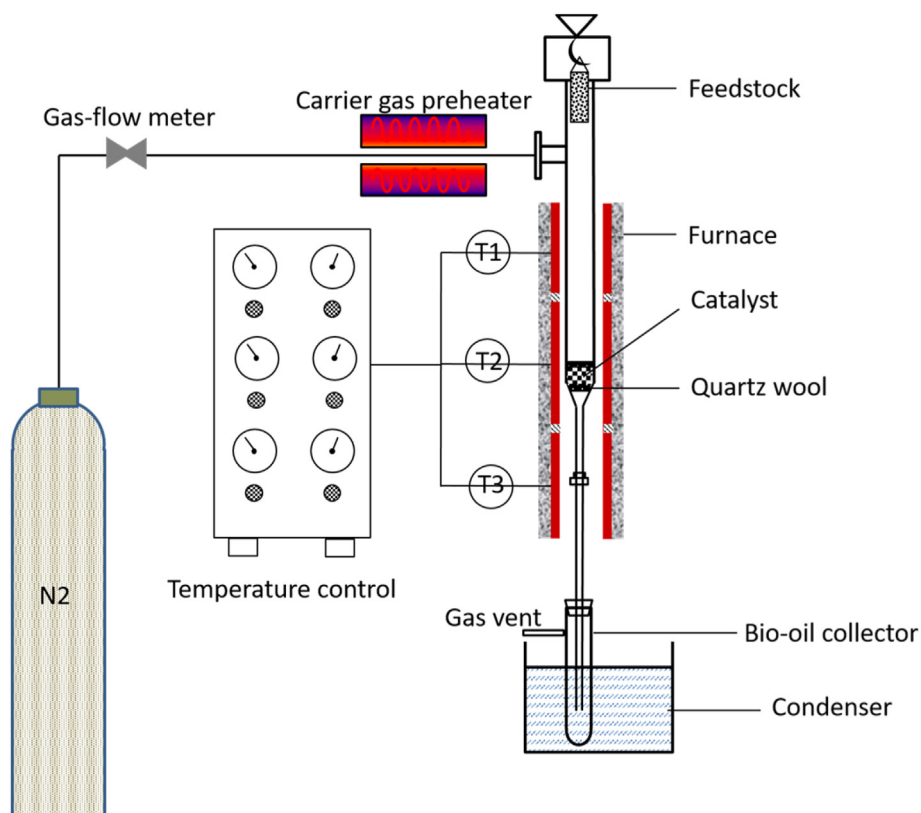


Fig. 1. Schematic diagram of ex-situ catalytic co-pyrolysis system.

280 °C, which was primarily due to the decomposition of hemicellulose, accompanied by small amounts of cellulose and lignin decomposition. A similar finding was reported by Phanphanich et al. [31]. On the other hand, the ash and fixed carbon contents of TPW were increased with the torrefaction temperature, similar to the study of Chen et al. [32]. As shown in Table 1, the content of hemicellulose was greatly reduced after 240 °C, indicating that thermal decomposition of hemicellulose occurred. The content of cellulose was not significantly influenced by the torrefaction due to the higher stability of cellulose, which mainly decomposed in the range of 350–450 °C [33]. The content of lignin was gradually increased from 16.78 to 40.83% when the torrefaction temperature rose from 0 to 280 °C. Similar results were observed by Zheng et al. [34], who proposed that the increasing lignin content of torrefied corncob with elevated torrefaction temperature was associated with the severe decomposition of hemicellulose and the cross-linking/charring of holocellulose to form lignin-like aromatic structures.

3.2. Catalyst characterization

Fig. 2 shows the properties of parent and hierarchical HZSM-5 zeolites. As shown in Fig. 2(a), HZSM-5 zeolite exhibited a typical MFI structure at 2θ of 7.9°, 8.8°, 23.06°, 23.9°, and 24.34°. As the concentration of alkaline increased, the corresponding peak intensity of hierarchical HZSM-5 exhibited an obvious reduction due to the partial desilication of HZSM-5 framework, which was consistent with previous studies [14]. When the concentration of alkaline increased to 0.4 mol/L, the XRD pattern of HZSM-5 changed greatly resulting in the disappearance of peaks at $2\theta = 7.9^\circ$ and 8.8° , indicating that high concentration of alkaline led to the collapse of HZSM-5 framework. The NH_3 -TPD curves displayed two distinct peaks at 150–250 °C and 300–450 °C, corresponding to the weak and strong acidity respectively (Fig. 2(c)). The strong acidity decreased as the concentration of NaOH increased, whereas the strength of weak acidic sites increased and the peaks shifted to higher temperatures. However, the strong and weak acidity of 0.4-HZSM-5 showed no clear distinct boundary due to the framework damage caused by high alkaline concentration.

The nitrogen physisorption isotherms showed that parent HZSM-5 exhibited a type of IV isotherm with no hysteresis loop (Fig. 2(b)), indicating that the parent zeolite was dominated by the microporous structure. However, an obvious hysteresis loop was observed after alkaline treatment with different concentrations, suggesting that some mesopores or macropores were introduced into the zeolite catalyst. The rapid increase in absorption may be caused by the capillary condensation due to the connection of mesopores surface with intracrystalline micropores [29]. The textural properties of the parent and hierarchical HZSM-5 are given in Table 2. The BET surface area of parent HZSM-5 was 324 m²/g

with dominant micropore surface area of 220 m²/g. As the concentration of alkaline increased, the BET surface area and total pore volume first increased and then decreased, reaching the maximum of 375 m²/g and 0.52 m³/g at 0.3 mol/L NaOH solution, respectively. The S_{meso} and V_{meso} showed the same trend with S_{BET} and V_{total} , while the S_{micro} and V_{micro} decreased with the increase of alkaline concentrations due to the development of the mesoporous structure. The results of the effect of alkaline treatment on zeolite textural properties were consistent with those previous studies [35,36].

3.3. Effect of torrefaction temperature on non-catalytic and catalytic co-pyrolysis

3.3.1. Product yield

The bio-oil, gas, and char yields obtained from co-pyrolysis of TPW/HDPE at various torrefaction temperatures are shown in Fig. 3(a). As the torrefaction temperature increased from 0 to 280 °C, the bio-oil yield was gradually decreased from 60.42% to 44.95%, reducing by 25.6%. In contrast, an increase in char yield was observed, which increased to 21.63% at the maximum torrefaction temperature of 280 °C. It can be seen that the torrefaction temperature has an important effect on the yield of co-pyrolysis products. With increasing torrefaction temperature, the moisture in PW was evaporated and the hemicellulose was decomposed due to its poor thermal stability, thereby reducing the bio-oil yield. This result was in accordance with Zhang et al. [37], who found that the bio-oil yield of torrefied biomass decreased while the yield of char increased with increasing torrefaction temperature. The increase in char yield may be related to the increasing polycondensation and charring of TPW at higher torrefaction temperature [38].

The effect of torrefaction temperature on product yield obtained from the ex-situ catalytic co-pyrolysis of TPW/HDPE over 0.3-HZSM-5 zeolite is shown in Fig. 3(b). The yield of bio-oil from catalytic co-pyrolysis of raw PW/HDPE was 48.68%, which was lower than that obtained from non-catalytic co-pyrolysis. It was due to the fact that the co-pyrolysis vapors were further cracked at the active sites of 0.3-HZSM-5 zeolite, resulting in a reduced bio-oil yield and increased non-condensable gas yield compared to the non-catalytic co-pyrolysis. With increasing torrefaction temperature, the catalytic co-pyrolysis yield of bio-oil was decreased to 38.32% at the maximum torrefaction temperature of 280 °C, indicating that torrefaction affected the product yield from catalytic co-pyrolysis. This result was in agreement with the study of Chen et al. [39]. The char yield obtained from catalytic co-pyrolysis was consistent with that from non-catalytic co-pyrolysis due to the ex-situ catalysis mode. The yield of coke formed in the 0.3-HZSM-5 zeolite after catalytic co-pyrolysis of raw PW/HDPE was 6.10%, and the torrefaction temperature had no significant effect on coke formation.

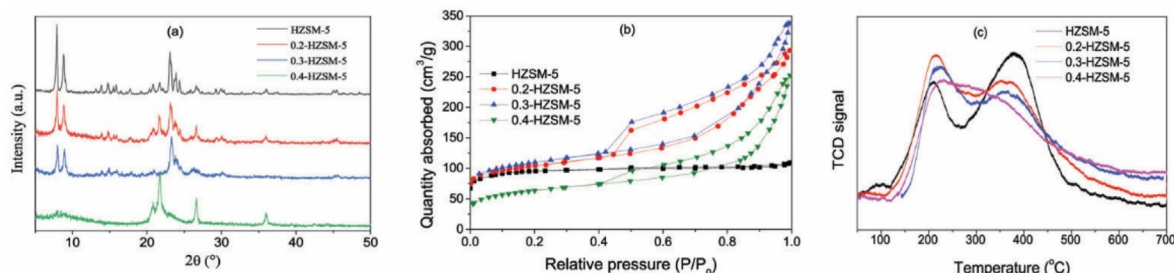


Fig. 2. Characterizations of parent and hierarchical HZSM-5 treated by various NaOH concentrations. (a) XRD patterns; (b) Nitrogen physisorption isotherms; (c) NH_3 -TPD curves.

Table 2
Textural properties of the parent and hierarchical HZSM-5 zeolites.

Samples	$S_{\text{BET}} / \text{m}^2 \cdot \text{g}^{-1}$	$S_{\text{micro}} / \text{m}^2 \cdot \text{g}^{-1}$	$S_{\text{meso}} / \text{m}^2 \cdot \text{g}^{-1}$	$V_{\text{total}} / \text{cm}^3 \cdot \text{g}^{-1}$	$V_{\text{micro}} / \text{cm}^3 \cdot \text{g}^{-1}$	$V_{\text{meso}} / \text{cm}^3 \cdot \text{g}^{-1}$	Pore size/nm
HZSM-5	324	220	104	0.17	0.10	0.07	2.08
0.2-HZSM-5	357	192	165	0.45	0.09	0.36	5.07
0.3-HZSM-5	375	182	193	0.52	0.09	0.43	5.26
0.4-HZSM-5	222	78	144	0.39	0.03	0.36	6.94

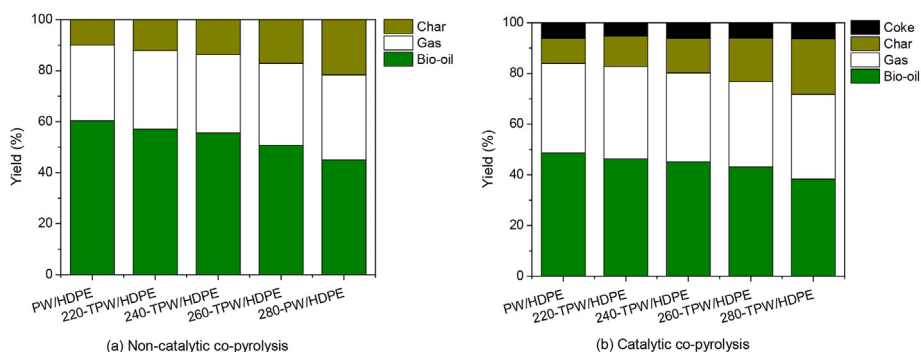


Fig. 3. Effect of torrefaction temperature on the product yield in (a) non-catalytic and (b) catalytic co-pyrolysis of TPW/HDPE over 0.3-HZSM-5.

3.3.2. Product distribution from non-catalytic co-pyrolysis

The co-pyrolysis of raw PW/HDPE mixture produced complex distribution of the products, including oxygenated compounds (acids, ketones, furans, phenols, anhydrosugars, etc.) derived from PW pyrolysis and hydrocarbon compounds (alkanes, alkenes, and alkadienes) derived from HDPE pyrolysis. TPW/HDPE had similar product distribution to raw PW/HDPE while their contents were different as shown in Table 3. Among the oxygenated compounds, a remarkable decrease of acids, furans, and anhydrosugars, which derived from the decomposition of holocellulose, was observed with the increase of the torrefaction temperature. On the other hand, the yield of phenols was significantly increased with torrefaction temperatures, reaching its maximum of 22.14% at 260 °C. A similar result was reported by Xin et al. [40], who found that torrefaction pretreatment of herbaceous residues reduced the content of oxygenated low molecular species (acid, ketones, and aldehydes) while increased phenols content. This was ascribed to the fact that the relative amounts of holocellulose and lignin in PW as well as their structures were significantly altered by torrefaction, resulting in the difference in oxygenated product distribution [41,42]. Notably, aromatic compounds were observed after torrefaction, and its yield was increased with the torrefaction temperature. The degradation of cellulose and hemicellulose followed by subsequent poly-condensation reactions during torrefaction may contribute to the formation of aromatics [43]. On the other hand, a gradual

Table 3
Effect of torrefaction temperature on the co-pyrolysis product distribution.

Group	Peak area (%)				
	0 °C	220 °C	240 °C	260 °C	280 °C
Acids	8.94	7.82	7.51	6.16	5.01
Ketones	6.54	7.01	7.28	6.56	5.72
Furans	5.29	3.56	2.68	1.84	2.06
Phenols	13.87	18.51	18.82	22.14	21.81
Anhydrosugars	4.83	2.64	3.17	1.81	0.57
Aromatics	0	1.99	2.75	4.73	5.87
Alkenes	35.21	36.06	38.93	40.27	39.57
Alkanes	10.80	8.08	7.05	6.43	6.95
Alkadienes	6.77	6.98	5.54	4.6	5.07

decrease in alkanes and alkadienes yield was found with an increase of the torrefaction temperature from 220 to 280 °C. Meanwhile, the yield of alkenes was increased with the torrefaction temperature. The increase in alkenes may be attributed to the fact that torrefaction promoted the hydrogen transfer reaction between lignin radicals and HDPE while inhibited the intermolecular hydrogen transfer reactions of HDPE [44]. Thereby, torrefaction pretreatment decreased the formation of alkanes and alkadienes while enhanced alkenes production.

The relative content of some typical oxygenated compounds changing with torrefaction temperatures are shown in Fig. 4. The increase in torrefaction temperature caused a significant reduction of acetic acid, which was mainly derived from the deacetylation of O-acetyl groups linked to the hemicellulose [45]. The obvious decrease of furfural with torrefaction was also largely due to the decomposition of hemicellulose since furfural was the most important ring-containing product from the hemicellulose pyrolysis [46]. Levoglucosan was mainly formed by the decomposition of a glycosidic bond of cellulose, and its decrease with torrefaction indicated the structural change in cellulose caused by torrefaction [41]. The phenolic compounds were mainly generated from lignin decomposition. As the torrefaction temperature increased, the yields of phenol, catechol, methyl phenols, and dimethyl phenols were increased. Meanwhile, the yields of guaiacol and 2,6-dimethoxy phenol were decreased. It suggested that the increase of torrefaction temperatures facilitated the formation of simple alkylphenols by promoting the cleavage of ether linkages and demethoxylation of lignin structure [43]. A similar trend was reported by Wang et al. [47], who observed that the yield of non-methoxylated phenols from lignin pyrolysis was increased after torrefaction.

3.3.3. Product distribution from catalytic co-pyrolysis

The major products identified from the catalytic co-pyrolysis of TPW/HDPE were classified into 7 groups as shown in Fig. 5(a): mono-aromatics, PAHs, alkanes, alkenes, alkadienes, oxygenates, and others. It can be seen that the product distribution was significantly changed after introducing 0.3-HZSM-5 zeolite as the catalyst. Previous studies have demonstrated that HZSM-5 zeolite

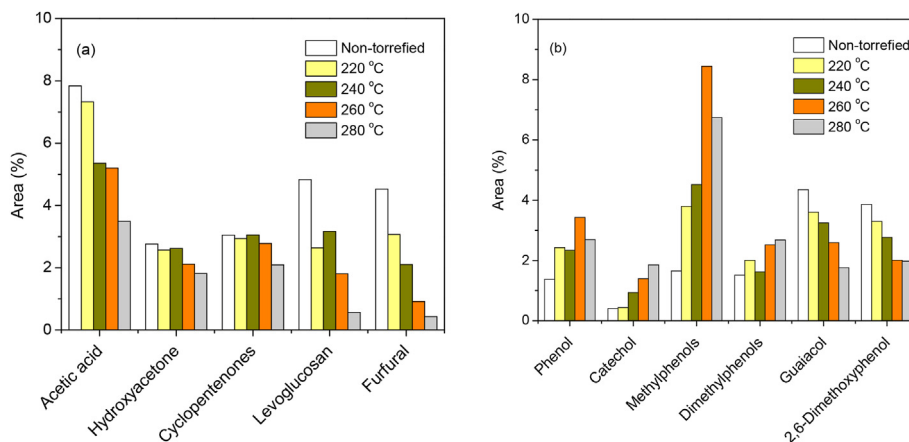


Fig. 4. Effect of torrefaction temperature on the yields of typical oxygenated compounds from non-catalytic co-pyrolysis of PW/HDPE. (a) Compounds from holocellulose; (b) compounds from lignin.

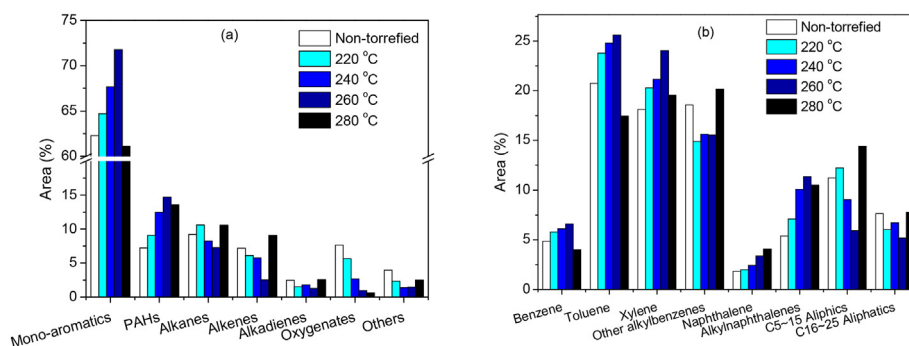


Fig. 5. Effect of torrefaction temperature on the product distribution from catalytic co-pyrolysis of PW/HDPE over 0.3-HZSM-5. (a) Product distribution; (b) Hydrocarbon distribution.

has good catalytic activity of deoxygenation and cracking, which could convert oxygenates (acids, furans, aldehydes, ketones, phenols, etc.) and alkenes into aromatics through a series of reactions [48–50]. As shown in Fig. 5(a), the yield of mono-aromatics from catalytic co-pyrolysis of raw PW/HDPE was 62.29%, which increased to 71.75% at 260 °C and then decreased with further increasing torrefaction temperature. The decrease of mono-aromatics at 280 °C may be related with the loss of cellulose [51]. The yield of PAHs exhibited a similar trend with mono-aromatics, which increased from 7.23% for raw PW/HDPE to 14.71% for 260-TPW/HDPE. One possible explanation for the higher aromatics yield may be associated with the structural change of cellulose and lignin by torrefaction as proposed by Park's group [19]. They found that torrefaction promoted the ring opening of cellulose leading to the enhanced production of aliphatic intermediates, which are the intermediates for the formation of aromatics. Another possible reason they proposed was that the synergistic effect such as Diels-Alder reaction in the production of aromatics from the catalytic co-pyrolysis of cellulose and polypropylene (PP) was promoted by torrefaction pretreatment [17]. On the other hand, the yield of aliphatic hydrocarbons (alkanes, alkenes, and alkadienes) decreased with increasing torrefaction temperature to 260 °C. The group of oxygenates (2-methylfuran, 2-cyclopentene-1-one, phenol, 3-methylphenol, etc.) was also reduced due to the combined effect of torrefaction and 0.3-HZSM-5 zeolite.

Fig. 5(b) shows the hydrocarbon product distribution from catalytic co-pyrolysis of TPW/HDPE at various torrefaction temperatures. The selectivities of benzene, toluene, and xylene were 4.85%,

20.73%, and 18.12%, respectively. As the torrefaction temperature increased, the BTX selectivities increased first and then decreased, reaching their maximum at 260 °C. For example, the selectivity of toluene increased from 20.73% to 25.60% as the torrefaction temperature increased from 0 to 260 °C and then decreased to 17.45% when the torrefaction temperature further increased to 280 °C. It is reported that BTX selectivities from catalytic fast pyrolysis of biomass components followed the order of lignin > hemicellulose > cellulose [52]. Thus, the increase in selectivities of BTX could be attributed to the increasing lignin content of TPW with the increase of torrefaction temperature. However, severe torrefaction temperature (280 °C) prompted the cross-linking and charring of TPW components to form carbonaceous structures which caused the increase of char yield and reduction of BTX selectivities. The selectivity of other alkylbenzenes, such as ethylbenzene, 1,2,3-trimethylbenzene, and 1-ethyl-2-methylbenzene, displayed an opposite trend with BTX. The result was in agreement with the study of Zheng et al. [34], who investigated the effect of torrefaction temperature on the selectivity of aromatics during the catalytic fast pyrolysis of corncob over HZSM-5. They found that the selectivity of alkylbenzenes first decreased and then increased as the torrefaction temperature increased [34]. On the other hand, the selectivity of aliphatic hydrocarbons, especially light aliphatics with carbon number in the range of C5–15, declined as the torrefaction temperature increased to 260 °C. It can be concluded that torrefaction favored the formation of BTX at the expense of aliphatic hydrocarbons. However, higher torrefaction temperature (280 °C) has a negative effect on the BTX selectivity.

3.4. Effect of alkaline concentration on the catalytic activity of hierarchical HZSM-5

The effect of alkaline concentration on the product distribution from catalytic co-pyrolysis of 260-TPW/HDPE is shown in Fig. 6. It can be seen that the catalytic co-pyrolysis of 260-TPW/HDPE with parent and hierarchical HZSM-5 zeolites produced predominantly aromatics (mono-aromatics and PAHs). As the alkaline concentration increased, the relative content of mono-aromatics increased from 63.79% for the parent HZSM-5 to 71.75% for 0.3-HZSM-5, while the content of mono-aromatics significantly decreased to 48.44% with further increasing the alkaline concentration. The content of PAHs exhibited a different trend with mono-aromatics, which decreased to 7.21% as the concentration of alkaline increased to 0.4 mol/L. The results indicated that alkaline concentration has an important effect on the aromatics production. The low alkaline concentration (≤ 0.3 mol/L) promoted the aromatization reactions of HZSM-5 catalyst, which led to an enhanced formation of mono-aromatics. However, the higher alkaline concentration destroyed the structure of HZSM-5 catalyst, resulting in the reduction of aromatics. Although alkaline treatment reduced the strong acid sites in HZSM-5, it increased the mesoporosity of the zeolite, improving the accessibility of the acid sites [53]. Thus, the bulky oxygenates and aliphatic hydrocarbons could easily diffuse into the mesopores of hierarchical HZSM-5 and efficiently use the acid sites to form aromatics. The reduction of PAHs was due to the fact that alkaline treatment decreased the diffusion path length of molecules in the hierarchical HZSM-5 zeolites, thereby inhibiting the secondary polymerization reactions of mono-aromatics [54]. Pérez-Ramírez et al. [55] also reported that the improved pyrolysis performance of polyethylene over hierarchical zeolites was attributed to the alleviated diffusion limitations and shorter diffusion path lengths. On the other hand, the content of aliphatic hydrocarbons (alkanes, alkenes, and alkadienes) and oxygenates decreased with increasing alkaline concentration to 0.3 mol/L, which probably entered the catalyst pores and underwent a series of reactions to form aromatics. The above results suggested that hierarchical HZSM-5 treated with appropriate alkaline concentration has higher diffusion and deoxygenation efficiency compared to parent HZSM-5, enhancing the production of valuable mono-aromatic hydrocarbons.

The selectivity of hydrocarbons was also affected by alkaline treatment of HZSM-5 as shown in Fig. 6(b). An obvious decrease in the selectivity of benzene and toluene were observed when the concentration of alkaline increased. The selectivity of benzene and toluene reduced from 7.72% to 0.7% and 32.08%–16.23%, respectively. On the contrary, the selectivity of xylenes and other alkylbenzenes first increased with increasing alkaline concentration to

0.3 mol/L, and decreased with further increasing alkaline concentration to 0.4 mol/L. The highest selectivity of xylenes and other alkylbenzenes reached 24.03% and 15.54% in the presence of 0.3-HZSM-5, respectively. The selectivity of naphthalene and alkyl-naphthalenes (1-methylnaphthalene, 1,2-dimethylnaphthalene, etc.) displayed downward trends with the increase in alkaline concentration, which reduced by 39.17% and 66.49%, respectively. This result was consistent with the study of Dai et al. [56], who observed that the selectivity of PAHs declined while the selectivity of alkylbenzenes increased after alkaline desilication of HZSM-5 zeolite. The selectivity of light aliphatic hydrocarbons also decreased from 9.35% to 5.90% when the concentration of alkaline increased from 0 to 0.3 mol/L. However, further increasing the alkaline concentration to 0.4 mol/L resulted in the higher selectivity of aliphatic hydrocarbons due to the destroyed pore structure of HZSM-5 zeolite. The above results indicated that hierarchical HZSM-5 treated with appropriate alkaline concentrations could promote the selectivity of mono-aromatics with larger dynamic diameters due to the enlarged pore structure.

3.5. Reaction mechanism

The reaction mechanism for catalytic co-pyrolysis of TPW/HDPE over hierarchical HZSM-5 zeolite is shown in Fig. 7. The torrefaction pretreatment is a deoxygenation process, which changed the relative contents and structures of cellulose, hemicellulose, and lignin in different degrees. It decomposed hemicellulose and small amounts of cellulose and lignin depending on the torrefaction temperature. Consequently, the formation of high oxygen-containing compounds (acetic acid, furfural, levoglucosan, etc.) was reduced. Moreover, the observed aromatics in co-pyrolysis of TPW/HDPE indicated that torrefaction may change the C–O–C and glucosidic bonds of cellulose leading to the ring opening of glucose structural units. The opening chain structure underwent dehydration, decarbonylation, arrangement and aromatization reactions to form aromatics [41]. Torrefaction increased the relative content of lignin due to the elimination of hemicellulose and promoted cleavage of ether linkages and demethoxylation reactions, leading to the enhanced production of phenol, catechol, and methyl phenols at the expense of guaiacyl and syringyl phenols. On the other hand, the thermal decomposition of HDPE follows a radical mechanism to form alkenes and alkadienes are generated by hydrogen transfer reactions [44,57]. During the co-pyrolysis process, torrefaction pretreatment may inhibited the intermolecular hydrogen transfer reactions resulting in an enhanced production of alkenes at the expense of alkanes and alkadienes. It can be concluded that torrefaction pretreatment improved the product distribution of TPW/HDPE co-pyrolysis. The improved co-pyrolysis

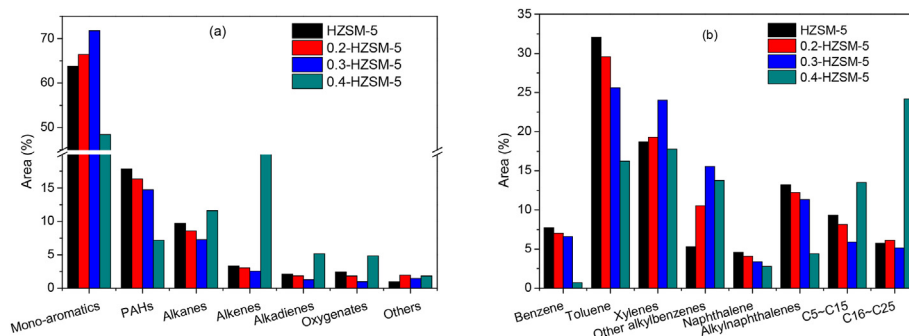


Fig. 6. Effect of hierarchical HZSM-5 treated with various alkaline concentrations on the product distribution from catalytic co-pyrolysis of 260-TPW/HDPE. (a) Product distribution; (b) Hydrocarbon distribution.

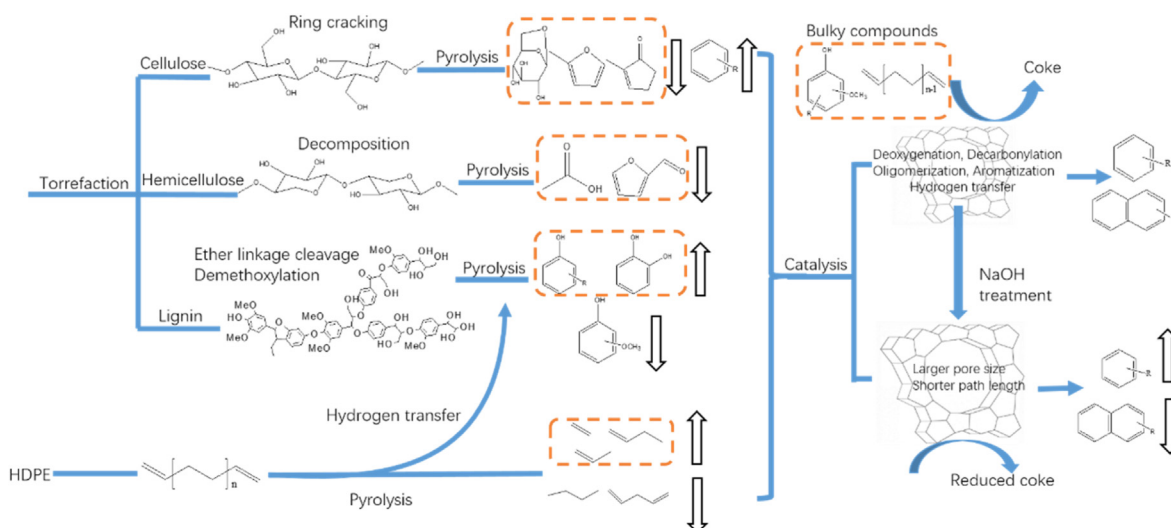


Fig. 7. The catalytic co-pyrolysis mechanism of TPW/HDPE over hierarchical HZSM-5.

vapors then diffused into the pores of HZSM-5 zeolite and underwent a series of deoxygenation and aromatization reactions to form aromatics. Some bulky compounds were limited to access into the pores and then deposited on the zeolite surface to form coke. The desilication of HZSM-5 treated by controlling alkaline concentration newly created large amounts of mesopores on the zeolite surface, improving the diffusion efficiency of bulky compounds. In addition, the shortened channel length by alkaline treatment inhibited secondary reactions such as polymerization, reducing the formation of PAHs. As a result, the hierarchical HZSM-5 produced more mono-aromatics during catalytic co-pyrolysis of TPW/HDPE compared with parent HZSM-5.

4. Conclusions

The catalytic co-pyrolysis of TPW and HDPE over hierarchical HZSM-5 was performed to produce value-added mono-aromatic hydrocarbons in a fixed bed reactor. Although torrefaction reduced bio-oil yield, it was demonstrated to be effective in deoxygenation of bio-oil compounds, favoring the formation of aromatics. Moreover, torrefaction promoted the hydrogen transfer reaction between lignin and HDPE, resulting in the increase of phenols and alkenes with torrefaction temperature. In the co-pyrolysis of TPW/HDPE over hierarchical HZSM-5, both the torrefaction temperature and alkaline concentration exhibited significant effects on the production of mono-aromatics as well as the selectivity of BTX. The amount of mono-aromatics reached the maximum of 71.75% at the torrefaction temperature of 260 °C over hierarchical HZSM-5 treated with 0.3 mol/L alkaline. Severe torrefaction temperature (280 °C) and alkaline concentration (0.4 mol/L) resulted in the decomposition of cellulose and the framework damage of zeolite respectively, which had a negative effect on aromatic production. It can be concluded that torrefaction coupled with hierarchical HZSM-5 catalysis is promising to enhance the production of value-added mono-aromatics from co-pyrolysis of biomass and plastic waste.

CRedit authorship contribution statement

Xiaona Lin: Conceptualization, Methodology, Writing - original draft. **Lingshuai Kong:** Investigation, Resources, Data curation. **Xiajin Ren:** Investigation, Data curation. **Donghong Zhang:**

Investigation, Resources, Data curation. **Hongzhen Cai:** Writing - review & editing. **Hanwu Lei:** Writing - review & editing.

Declaration of competing interest

The authors declare that they have no known competing financial interests or personal relationships that could have appeared to influence the work reported in this paper.

Acknowledgments

The authors are grateful for financial support from the National Natural Science Foundation of China (51806129), and the Natural Science Foundation of Shandong Province of China (ZR2017BEE062), the Agriculture and Food Research Initiative Competitive Grant no. 2016-67021-24533 and 2014-38502-22598 from the National Institute of Food and Agriculture, United States Department of Agriculture.

References

- [1] K.G. Kalogiannis, S.D. Stefanidis, S.A. Karakoulia, K.S. Triantafyllidis, H. Yiannoulakis, C. Michailof, A.A. Lappas, First pilot scale study of basic vs acidic catalysts in biomass pyrolysis: deoxygenation mechanisms and catalyst deactivation, *Appl. Catal. B Environ.* 238 (2018) 346–357.
- [2] Y. Xue, X. Bai, Synergistic enhancement of product quality through fast co-pyrolysis of acid pretreated biomass and waste plastic, *Energy Convers. Manag.* 164 (2018) 629–638.
- [3] Q. Zhang, J. Chang, T. Wang, Y. Xu, Review of biomass pyrolysis oil properties and upgrading research, *Energy Convers. Manag.* 48 (2007) 87–92.
- [4] A. Ephraim, D. Pham Minh, D. Lebonnois, C. Peregrina, P. Sharrock, A. Nzihou, Co-pyrolysis of wood and plastics: influence of plastic type and content on product yield, gas composition and quality, *Fuel* 231 (2018) 110–117.
- [5] W. Chen, S. Shi, J. Zhang, M. Chen, X. Zhou, Co-pyrolysis of waste newspaper with high-density polyethylene: synergistic effect and oil characterization, *Energy Convers. Manag.* 112 (2016) 41–48.
- [6] Q. Bu, Y. Liu, J. Liang, H.M. Morgan, L. Yan, F. Xu, H. Mao, Microwave-assisted co-pyrolysis of microwave torrefied biomass with waste plastics using ZSM-5 as a catalyst for high quality bio-oil, *J. Anal. Appl. Pyrol.* 134 (2018) 536–543.
- [7] Y. Zhang, D. Duan, H. Lei, E. Villota, R. Ruan, Jet fuel production from waste plastics via catalytic pyrolysis with activated carbons, *Appl. Energy* 251 (2019) 113337.
- [8] M.J.C. van der Stelt, H. Gerhauser, J.H.A. Kiel, K.J. Ptasiński, Biomass upgrading by torrefaction for the production of biofuels: a review, *Biomass Bioenergy* 35 (2011) 3748–3762.
- [9] D. Chen, A. Gao, K. Cen, J. Zhang, X. Cao, Z. Ma, Investigation of biomass torrefaction based on three major components: hemicellulose, cellulose, and lignin, *Energy Convers. Manag.* 169 (2018) 228–237.
- [10] H.W. Lee, Y.-M. Kim, B. Lee, S. Kim, J. Jae, S.-C. Jung, T.-W. Kim, Y.-K. Park,

- Catalytic copyrolysis of torrefied cork oak and high density polyethylene over a mesoporous HY catalyst, *Catal. Today* 307 (2018) 301–307.
- [11] D. Chen, Z. Zheng, K. Fu, Z. Zeng, J. Wang, M. Lu, Torrefaction of biomass stalk and its effect on the yield and quality of pyrolysis products, *Fuel* 159 (2015) 27–32.
 - [12] A. Álvarez, D. Nogueiro, C. Pizarro, M. Matos, J.L. Bueno, Non-oxidative torrefaction of biomass to enhance its fuel properties, *Energy* 158 (2018) 1–8.
 - [13] Y. Yue, H. Singh, B. Singh, S. Mani, Torrefaction of sorghum biomass to improve fuel properties, *Bioresour. Technol.* 232 (2017) 372–379.
 - [14] L. Dai, Y. Wang, Y. Liu, R. Ruan, D. Duan, Y. Zhao, Z. Yu, L. Jiang, Catalytic fast pyrolysis of torrefied corn cob to aromatic hydrocarbons over Ni-modified hierarchical ZSM-5 catalyst, *Bioresour. Technol.* 272 (2019) 407–414.
 - [15] A.J. Foster, J. Jae, Y.-T. Cheng, G.W. Huber, R.F. Lobo, Optimizing the aromatic yield and distribution from catalytic fast pyrolysis of biomass over ZSM-5, *Appl. Catal. Gen.* 423–424 (2012) 154–161.
 - [16] T.R. Carlson, G.A. Tompsett, W.C. Conner, G.W. Huber, Aromatic production from catalytic fast pyrolysis of biomass-derived feedstocks, *Top. Catal.* 52 (2009) 241–252.
 - [17] H.W. Lee, Y.-M. Kim, J. Jae, J.-K. Jeon, S.-C. Jung, S.C. Kim, Y.-K. Park, Production of aromatic hydrocarbons via catalytic co-pyrolysis of torrefied cellulose and polypropylene, *Energy Convers. Manag.* 129 (2016) 81–88.
 - [18] E.B. Hassan, I. Elsayed, A. Eseyin, Production high yields of aromatic hydrocarbons through catalytic fast pyrolysis of torrefied wood and polystyrene, *Fuel* 174 (2016) 317–324.
 - [19] Y.-M. Kim, J. Jae, B.-S. Kim, Y. Hong, S.-C. Jung, Y.-K. Park, Catalytic co-pyrolysis of torrefied yellow poplar and high-density polyethylene using microporous HZSM-5 and mesoporous Al-MCM-41 catalysts, *Energy Convers. Manag.* 149 (2017) 966–973.
 - [20] R. French, S. Czernik, Catalytic pyrolysis of biomass for biofuels production, *Fuel Process. Technol.* 91 (2010) 25–32.
 - [21] C. Hu, R. Xiao, H. Zhang, Ex-situ catalytic fast pyrolysis of biomass over HZSM-5 in a two-stage fluidized-bed/fixed-bed combination reactor, *Bioresour. Technol.* 243 (2017) 1133–1140.
 - [22] Y. Lin, C. Zhang, M. Zhang, J. Zhang, Deoxygenation of bio-oil during pyrolysis of biomass in the presence of CaO in a fluidized-bed reactor, *Energy Fuels* 24 (2010) 5686–5695.
 - [23] V.B. Custodis, S.A. Karakoulia, K.S. Triantafyllidis, J.A. van Bokhoven, Catalytic fast pyrolysis of lignin over high-surface-area mesoporous aluminosilicates: effect of porosity and acidity, *ChemSusChem* 9 (2016) 1134–1145.
 - [24] Y. Zhang, H. Lei, Z. Yang, D. Duan, E. Villota, R. Ruan, From glucose-based carbohydrates to phenol-rich bio-oils integrated with syngas production via catalytic pyrolysis over an activated carbon catalyst, *Green Chem.* 20 (2018) 3346–3358.
 - [25] Q. Lu, M. Zhou, W. Li, X. Wang, M. Cui, Y. Yang, Catalytic fast pyrolysis of biomass with noble metal-like catalysts to produce high-grade bio-oil: analytical Py-GC/MS study, *Catal. Today* 302 (2018) 169–179.
 - [26] H. Hernando, I. Moreno, J. Feroso, C. Ochoa-Hernández, P. Pizarro, J.M. Coronado, J. Čejka, D.P. Serrano, Biomass catalytic fast pyrolysis over hierarchical ZSM-5 and Beta zeolites modified with Mg and Zn oxides, *Biomass Convers. Biorefinery* 7 (2017) 289–304.
 - [27] G.T. Neumann, J.C. Hicks, Novel hierarchical cerium-incorporated MFI zeolite catalysts for the catalytic fast pyrolysis of lignocellulosic biomass, *ACS Catal.* 2 (2012) 642–646.
 - [28] J. Li, X. Li, G. Zhou, W. Wang, C. Wang, S. Komarneni, Y. Wang, Catalytic fast pyrolysis of biomass with mesoporous ZSM-5 zeolites prepared by desilication with NaOH solutions, *Appl. Catal. Gen.* 470 (2014) 115–122.
 - [29] H. Chen, H. Cheng, F. Zhou, K. Chen, K. Qiao, X. Lu, P. Ouyang, J. Fu, Catalytic fast pyrolysis of rice straw to aromatic compounds over hierarchical HZSM-5 produced by alkali treatment and metal-modification, *J. Anal. Appl. Pyrol.* 131 (2018) 76–84.
 - [30] S. Zhang, H. Zhang, X. Liu, S. Zhu, L. Hu, Q. Zhang, Upgrading of bio-oil from catalytic pyrolysis of pretreated rice husk over Fe-modified ZSM-5 zeolite catalyst, *Fuel Process. Technol.* 175 (2018) 17–25.
 - [31] M. Phanphanich, S. Mani, Impact of torrefaction on the grindability and fuel characteristics of forest biomass, *Bioresour. Technol.* 102 (2011) 1246–1253.
 - [32] D. Chen, K. Cen, X. Jing, J. Gao, C. Li, Z. Ma, An approach for upgrading biomass and pyrolysis product quality using a combination of aqueous phase bio-oil washing and torrefaction pretreatment, *Bioresour. Technol.* 233 (2017) 150–158.
 - [33] Y.-C. Lin, J. Cho, G.A. Tompsett, P.R. Westmoreland, G.W. Huber, Kinetics and mechanism of cellulose pyrolysis, *J. Phys. Chem. C* 113 (2009) 20097–20107.
 - [34] A. Zheng, Z. Zhao, Z. Huang, K. Zhao, G. Wei, X. Wang, F. He, H. Li, Catalytic fast pyrolysis of biomass pretreated by torrefaction with varying severity, *Energy Fuels* 28 (2014) 5804–5811.
 - [35] J.C. Groen, W. Zhu, S. Brouwer, S.J. Huynink, F. Kapteijn, J.A. Moulijn, J. Pérez-Ramírez, Direct demonstration of enhanced diffusion in mesoporous ZSM-5 zeolite obtained via controlled desilication, *J. Am. Chem. Soc.* 129 (2007) 355–360.
 - [36] X. Zhu, L.L. Lobban, R.G. Mallinson, D.E. Resasco, Tailoring the mesopore structure of HZSM-5 to control product distribution in the conversion of propanal, *J. Catal.* 271 (2010) 88–98.
 - [37] H. Zhang, S. Shao, Y. Jiang, T. Vitidsant, P. Reubroycharoen, R. Xiao, Improving hydrocarbon yield by two-step pyrolysis of pinewood in a fluidized-bed reactor, *Fuel Process. Technol.* 159 (2017) 19–26.
 - [38] A. Zheng, L. Jiang, Z. Zhao, Z. Huang, K. Zhao, G. Wei, X. Wang, F. He, H. Li, Impact of torrefaction on the chemical structure and catalytic fast pyrolysis behavior of hemicellulose, lignin, and cellulose, *Energy Fuels* 29 (2015) 8027–8034.
 - [39] D. Chen, Y. Li, M. Deng, J. Wang, M. Chen, B. Yan, Q. Yuan, Effect of torrefaction pretreatment and catalytic pyrolysis on the pyrolysis poly-generation of pine wood, *Bioresour. Technol.* 214 (2016) 615–622.
 - [40] S. Xin, T. Mi, X. Liu, F. Huang, Effect of torrefaction on the pyrolysis characteristics of high moisture herbaceous residues, *Energy* 152 (2018) 586–593.
 - [41] V. Srinivasan, S. Adhikari, S.A. Chattanathan, M. Tu, S. Park, Catalytic pyrolysis of raw and thermally treated cellulose using different acidic zeolites, *Bio-Energy Res.* 7 (2014) 867–875.
 - [42] J. Meng, J. Park, D. Tilotta, S. Park, The effect of torrefaction on the chemistry of fast-pyrolysis bio-oil, *Bioresour. Technol.* 111 (2012) 439–446.
 - [43] S. Neupane, S. Adhikari, Z. Wang, A.J. Ragauskas, Y. Pu, Effect of torrefaction on biomass structure and hydrocarbon production from fast pyrolysis, *Green Chem.* 17 (2015) 2406–2417.
 - [44] E. Jakab, G. Varhegyi, O. Faix, Thermal decomposition of polypropylene in the presence of wood-derived materials, *J. Anal. Appl. Pyrol.* 56 (2000) 273–285.
 - [45] G. Lv, S. Wu, Analytical pyrolysis studies of corn stalk and its three main components by TG-MS and Py-GC/MS, *J. Anal. Appl. Pyrol.* 97 (2012) 11–18.
 - [46] C. Dong, Z. Zhang, Q. Lu, Y. Yang, Characteristics and mechanism study of analytical fast pyrolysis of poplar wood, *Energy Convers. Manag.* 57 (2012) 49–59.
 - [47] G. Dai, Q. Zou, S. Wang, Y. Zhao, L. Zhu, Q. Huang, Effect of torrefaction on the structure and pyrolysis behavior of lignin, *Energy Fuels* 32 (2017) 4160–4166.
 - [48] Y.-T. Cheng, G.W. Huber, Chemistry of furan conversion into aromatics and olefins over HZSM-5: a model biomass conversion reaction, *ACS Catal.* 1 (2011) 611–628.
 - [49] C. Dorado, C.A. Mullen, A.A. Boateng, H-ZSM5 catalyzed co-pyrolysis of biomass and plastics, *ACS Sustain. Chem. Eng.* 2 (2014) 301–311.
 - [50] Y. Wang, Q. Huang, Z. Zhou, J. Yang, F. Qi, Y. Pan, Online study on the pyrolysis of polypropylene over the HZSM-5 zeolite with photoionization time-of-flight mass spectrometry, *Energy & Fuels*, 2015, pp. 1090–1098.
 - [51] Z. Yang, A. Kumar, A.W. Apblett, A.M. Moneeb, Co-Pyrolysis of torrefied biomass and methane over molybdenum modified bimetallic HZSM-5 catalyst for hydrocarbons production, *Green Chem.* 19 (2017) 757–768.
 - [52] A. Zheng, Z. Zhao, S. Chang, Z. Huang, H. Wu, X. Wang, F. He, H. Li, Effect of crystal size of ZSM-5 on the aromatic yield and selectivity from catalytic fast pyrolysis of biomass, *J. Mol. Catal. Chem.* 383–384 (2014) 23–30.
 - [53] M.S. Holm, S. Svelle, F. Joensen, P. Beato, C.H. Christensen, S. Bordiga, M. Bjørgen, Assessing the acid properties of desilicated ZSM-5 by FTIR using CO and 2,4,6-trimethylpyridine (collidine) as molecular probes, *Appl. Catal. Gen.* 356 (2009) 23–30.
 - [54] C. Mei, P. Wen, Z. Liu, H. Liu, Y. Wang, W. Yang, Z. Xie, W. Hua, Z. Gao, Selective production of propylene from methanol: mesoporosity development in high silica HZSM-5, *J. Catal.* 258 (2008) 243–249.
 - [55] J. Pérez-Ramírez, S. Abelló, A. Bonilla, J.C. Groen, Tailored mesoporosity development in zeolite crystals by partial detemplation and desilication, *Adv. Funct. Mater.* 19 (2009) 164–172.
 - [56] G. Dai, S. Wang, Q. Zou, S. Huang, Improvement of aromatics production from catalytic pyrolysis of cellulose over metal-modified hierarchical HZSM-5, *Fuel Process. Technol.* 179 (2018) 319–323.
 - [57] A. Durmuş, S. Naci Koç, G. Selda Pozan, A. Kaşgöz, Thermal-catalytic degradation kinetics of polypropylene over BEA, ZSM-5 and MOR zeolites, *Appl. Catal. B Environ.* 61 (2005) 316–322.